Available online at www.sciencedirect.com
ScienceDirect
Applied Thermal Engineering 27 (2007) 2536–2548
Applied Thermal Engineering
www.elsevier.com/locate/apthermeng

Numerical investigation of the intercooler of a two-stage refrigerant compressor

Jeng-Min Huang [a,*], Chung-Ping Chiang [b], Jiing-Fu Chen [b], Yung-Lo Chow [b], Chi-Chuan Wang [b]

[a] Department of Refrigeration and Air-Conditioned, National Chin-Yi Institute of Technology, 35, Lane 215, Section 1, Chung-Shan Road, Taiping City, Taichung County 411, Taiwan
[b] Industrial Technology Research Institute, 195, Section 4, Chung-Hsing Road, Chutung, Hsinchu City 310, Taiwan

Received 20 November 2006; accepted 29 January 2007
Available online 13 February 2007

Abstract

This study performs a numerical study to examine the flow mixing characteristics subject to slot-injection and hole-injection of an intercooler applicable to a two-stage refrigerant compressor. The effect of injected angle and velocity is also investigated. The result indicates that the temperature distribution of a hole-injection is more uniform while the velocity distribution less uniform at a vertically injected arrangement. Larger injection angles generate bigger flow separation zones which results in velocity non-uniformity, whereas smaller injection angles give rise to a less velocity non-uniformity. As the injection velocity rises, both the temperature and velocity non-uniformity of the slot-injection type increase significantly whereas the injection velocity has negligible influence on the relevant uniformity for a hole-injection type. It is also found that the existence of the secondary vortices allows the hole-injection type to have a more uniform temperature and velocity distribution than that of the slot-injection type.

Keywords: Intercooler of a two-stage compressor; Mixing characteristic; CFD

1. Introduction

With the strong need of efficient energy use faced presently, the demand on high COP of centrifugal refrigerant compressors is increasing in recent HVAC&R applications. Single-stage compressors have already reached its potential limit since its COP can hardly be increased at all. In this regard, the exploitation of two-stage centrifugal compressors to increase overall COP becomes a very common way to achieve the goal. With the aid of a second expansion valve, the COP of two-stage centrifugal refrigerant compressors can be significantly improved due to reduction of the refrigerant temperature. The two-stage compressing process features an interstage liquid flash cooling as shown in Fig. 1. Part of the cold refrigerant vapor from the flash chamber is used to cool down the hot refrigerant vapor from the first compression by direct mixing. The well mixing vapor then enters the second stage impeller. A typical design for mixing of these two streams is schematically shown in Fig. 2a. The injected positions of the cold refrigerant are usually located on the interior of deswirl vanes or on the exit of deswirl vanes. The injecting the coolant near the inlet in deswirl vanes gives rise to well mixing of hot and cold streams. However, the disadvantage is to increase the aerodynamic loss and the uncertainty in the design of deswirl vanes. Injecting the coolant after exiting deswirl vanes or near the outlet in deswirl vanes have little effect on the angle design and performance of deswirl vanes, but the mixing of the cold and hot vapor will be less uniform.

Many numerical and experimental researches were conducted for film cooling which were related to the present

* Corresponding author. Tel.: +886 4 23924505; fax: +886 4 23932758.
E-mail address: jmh@ncit.edu.tw (J.-M. Huang).

1359-4311/$ - see front matter © 2007 Elsevier Ltd. All rights reserved.
doi:10.1016/j.applthermaleng.2007.01.028

Nomenclature

x	distance along direction of main stream
w	slot width
Pb	scaled pressure coefficient, defined in Eq. (1)
d	position of hole edge, shown in Fig. 2(c)
X	$(x-d)/w$
T	temperature
T_0	temperature of hot refrigerant
T_i	temperature of cold refrigerant
V_0	inlet velocity of hot refrigerant
V_i	average injected velocity
TSD	dimensionless temperature standard deviation of a cross-section
VSD	dimensionless velocity standard deviation of a cross-section
p_0	static pressure of hot refrigerant
p_i	static pressure of coolant
θ	injection angle, reference to streamwise direction
Cd	intercooler pressure loss coefficient,$= 0.5\Delta p/\rho V_0^2$
Δp	pressure drop from inlet to outlet of intercooler
ρ	density of refrigerant

study to some extent. For example, Fitt et al. [1] measured the downstream pressure distribution along the wall for an injection slot subject to the influence of blowing rates. Goldstein [2] conducted a flow visualization experiment for a film cooling flow near the end wall of a gas turbine. Ligrani et al. [3,4] measured the discharge coefficient of an injection hole and its adiabatic effectiveness. Schwarz and Goldstein [5] measured the film cooling effectiveness of a concave surface pertaining to the effects of hole diameter, density ratios, and blowing rates. Ligrani and Mitchell [6], Ekkad et al. [7], Nasir et al. [8], Lin and Shih [9], Lee et al. [10], Maiteh and Jubran [11], Yuen and Martinez-Botas [12] investigated the effects of streamwise and lateral angles on the film cooling effectiveness of a flat surface. The results showed that certain combination of hole diameter and angle could augment the cooling effectiveness and heat transfer coefficient. Considerable efforts were devoted to the effect of pulsating bulk flow on the heat transfer coefficient and effectiveness [13–18] for film cooling. The general conclusion is that the effect of turbulent intensity becomes weaker at a higher injection rate. Kim and Kim [19] performed a flow visualization experiment to examine the influence of configuration of injection hole on the cooling effectiveness of a leading edge film.

Some researches numerically investigated the film cooling phenomena. Amer et al. [20] used three turbulent models (k–ω model, modified k–ω model and k–ε model) to calculate two rows film cooling effectiveness. Their calculations were compared with the experimental data; showing turbulent model depends heavily on the blowing rate as well as on the distance downstream from the injection holes. Kadja and Bergeles [21] performed a 2D simulation of a slot-injection turbine blade cooling against the experimental data from Fitt et al. [1]. Bellettre et al. [22] used numerical method to calculate heat and mass transfer of several cooling media in the boundary layer and inside a plane porous plate. The turbulent model they applied was k–ε RNG model. Power-law scheme was used to discretize the convective term and the SIMPLE scheme was adopted to process pressure–velocity iteration. Lakehel et al. [23] used two kinds of turbulent models to simulate the flow field of turbine blade leading edge film cooling and compare with experimental data. Their results showed that the accuracy of two-layer model was better than standard k–ε model. Thakur et al. [24] used the standard k–ε model and a low Reynolds number model to investigate film cooling phenomena near the leading edge of a turbine blade. After comparing the temperature field with experimental

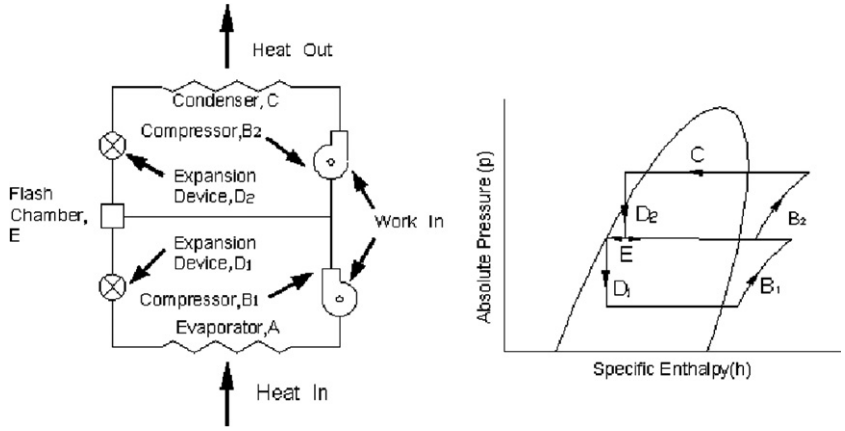

Fig. 1. A schematic of a two-stage compression system and its associated p–h diagram.

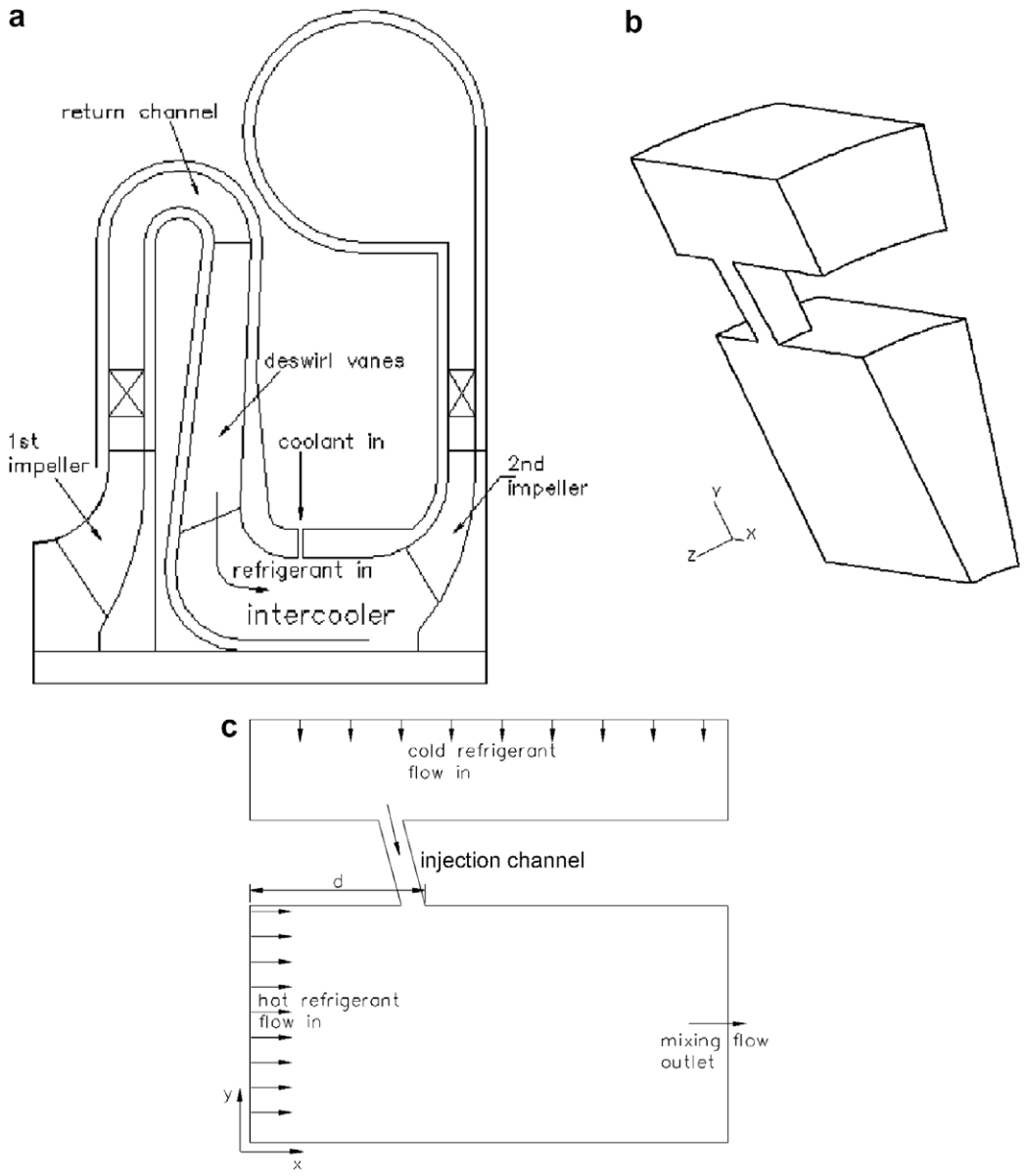

Fig. 2. (a) Diagram of the compressor's flow channel; (b) geometry of a hole-injection type; (c) geometry of a slot-injection type.

data, it is found that the low Reynolds number model gave better predictive ability than the standard model. Garg and Gaugler [25] used CFD to calculate the film cooling effectiveness of a rotating turbine blade. Garg [26] used k–ω model, q–ω model and Baldwin–Lomax model to calculate the heat transfer coefficient of film-cooled rotating blade. After comparing with the experimental data, they reported that the Baldwin–Lomax model was the most accurate one at the leading edge while k–ω model showed the best prediction on the pressure side of blade. In short, the k–ω model was better than the other two models. Koc et al. [27] used Fluent package to calculate the film cooling effectiveness subject to the influences of different rectangular holes, blowing rates and curvatures of surface. The turbulent model they applied was the standard k–ε model. Guo et al. [28] used large-eddy simulation model to compute the detailed flow field of film cooling. Miao and Wu [29] used low Reynolds number model to calculate the effect of hole shape on flat plate film cooling effectiveness. The research of film cooling focused on how to prevent hot gas from harming the surface of solids.

The foregoing studies are generally associated with the film cooling of turbine blades. However, there were no available studies associated with the uniformity of two mixing flow of two-stage compressing cycle in connection with the influence of temperature. It is evident from previous film cooling studies that the flow field has a strong impact on the overall performance. In this regard, it is the objective of this study to examine the mixing characteristics on the overall performance of a two-stage compression cycle. Two different types of injections, namely the hole-injection and slot-injection are systematically investigated.

This study will perform a more thorough analysis on this type of intercooler. In conventional design, it is often assumed that the cold and hot refrigerants are completely mixed before entering the second stage impeller and only the bulk temperature and velocity are used for further calculation. However, both temperatures and velocities should have different distributions at various designs of injection angles or blowing rates which may give rise to performance variation at the second stage compression. The present study aims to examine the level of mixing on the overall performance. There are two types of injection designs being investigated in this study. One is hole-injection type (3-D flow field) and the other is slot-injection type (2-D flow field).

2. Physical model, equations and methodology

The intercooler being investigated in this study is shown in Fig. 2a. Part of the refrigerant vapor after the first compression will be directed into the intercooler. This research adopts a typical geometry similar to a 500RT two-stage centrifugal refrigerant compressor as the basic design. The refrigerant is R-134a. Basic assumptions are as follows:

1. The flow is incompressible. The exiting static pressure of first stage is 581.4 kPa and the temperature is 25.05 °C. The pressure of the coolant is about 589 kPa and the temperature is 20.95 °C.
2. The physical properties of refrigerant vapor including thermal conductivity, molecular viscosity and specific heat are evaluated at constant pressures.
3. The velocity and temperature of the hot refrigerant vapor exiting deswirl vanes are uniformly distributed. However, the velocity distribution of the hot refrigerant vapor will not be uniform after passing through deswirl vanes. A better design of the channel curvature and deswirl vanes blade angles will reduce the non-uniformity of velocity field at the exit of deswirl vanes.
4. The velocity distribution from slot-injection type intercooler is axis-symmetrically distributed.
5. The shape of hole is rectangular for simplification.
6. The flow rates of coolant are about 6.5% and 10% of hot refrigerant flow rate.

With the preceding assumptions, the geometries shown in Fig. 2b and c were used for numerical computation. This study uses Star-CD software to simulate the temperature and flow fields. Conservation equations used for this study include the "continuity equation", the "turbulent momentum equations" and the "turbulent energy equations". The boundary conditions are as follows:

1. There are two inlets in computational domain. One is for the hot vapor which can be seen in Fig. 2 with a uniform inlet velocity of 21.5 m/s. The other one is specified for the injected cold vapor inlet as shown in Fig. 2c. The turbulent intensities in these two inlets are 0.05. The normal width of slot at entrance of intercooler is 4.65 mm. There are 13 holes at the entrance of intercooler and each of them has a normal area of 196 mm^2. The inlet total areas of the cooler are the same for slot-injection and hole-injection types. For comparison purpose, the basic conditions of hole-injection and slot-injection types are under the same injected mass flow rate and injected area. Due to the fixed density assumption, the cooler's velocity at the entrance of intercooler for these two types are the same.
2. The cross-section of the intercooler where the refrigerant leaves is regarded as an "outlet" boundary condition.

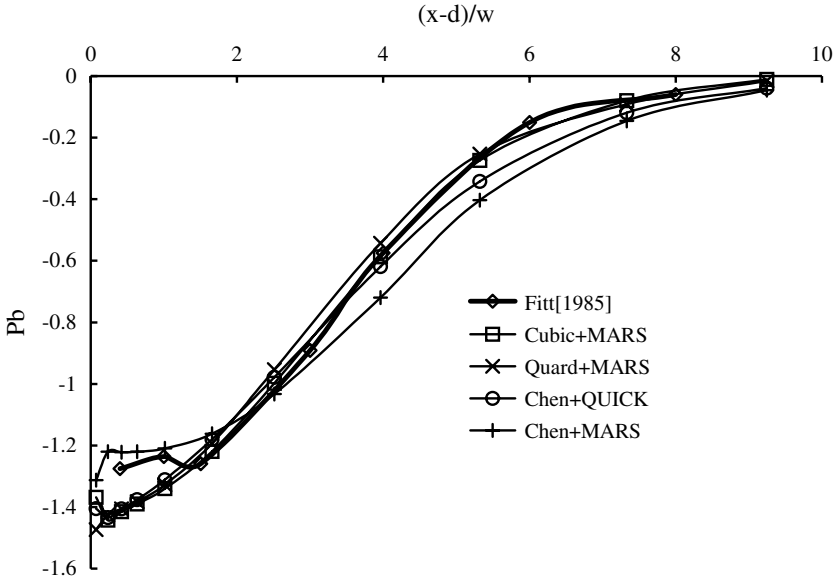

Fig. 3. Comparison from different turbulent models with experimental data from Fitt et al. [1].

3. The surfaces normal to circumferential direction are considered as a "symmetry" boundary condition.
4. The solid surfaces are termed as "smooth wall" surfaces.

As the flow field in film cooling of this study is very complex. Therefore, previous researches such as Amer et al. [20], Lakehel et al. [23], Thakur et al. [24], Garg [26], and Miao and Wu [29] all adopted different turbulent models to simulate the flow field. For substantiating the proposed turbulent modeling, a preliminary study is performed in comparison with the experimental data by Fitt et al. [1]. The experimental results of Fitt et al. [1] contains various injection velocity, this study only compares with the result from the largest injection velocity because it is similar to the ordinarily operational condition of an intercooler. The comparisons are shown in Fig. 3. The ordinate in Fig. 3 is Pb and is defined as:

$$\mathrm{Pb} = \frac{1}{B^{2/3}}\left(\frac{p_w - p_0}{p_{t0} - p_0}\right) \tag{1}$$

where B is the blowing rate, p_w is static pressure on the wall, p_0 is the static pressure at upstream of injection hole, and p_{t0} is the total pressure at upstream of injection hole. As seen in the figure, good agreement with the experimental data are shown, including (k–ε Chen's model + MARS), (k–ε Chen's model + QUICK), (k–ε/cubic/high Reynolds number model + MARS) and (k–ε/quadratic/high Reynolds number model + MARS). The plot of (k–ε Chen's model + MARS) shows the best agreement against experimental data in the constant pressure region, but has a larger deviation in the pressure distribution further downstream. Alternatively, the k–ε/cubic/ high Reynolds number model + MARS reveal a larger error in the constant pressure region, but coincide with the data in the pressure distribution downstream. The overall evaluation indicates that the k–ε/cubic/high Reynolds number model combined with the MARS method will be the most appropriate one in the present study. In this study, the SIMPLE scheme will be utilized for the iteration procedure and the convergence criterion is met when the residual values of velocities, pressure, temperature, and turbulent kinetic energy are all less than 10^{-4}. A nonlinear high Reynolds number turbulent model is applied in this study and the velocity near the wall surface is modeled by the "wall function". The consideration of laminar sub-layer is not necessary when y^+ is higher than 25. Note that y^+ for all solid wall in this study are all higher than 25.

The temperature and the velocity field may become unevenly distributed after the mixing of two refrigerant vapors. For evaluation of the uniformity of the temperature and velocity distribution, the standard deviation of the cross-sectional temperatures and velocities along the main stream is exploited as an indicator. The corresponding definition is as follows:

$$\mathrm{TSD} = \frac{1}{(T_0 - T_i)}\left[\frac{1}{N}\sum_{j=1}^{N}(T_j - T_a)^2\right]^{0.5} \tag{2}$$

$$\mathrm{VSD} = \frac{1}{V_0}\left[\frac{1}{N}\sum_{j=1}^{N}(V_j - V_a)^2\right]^{0.5} \tag{3}$$

TSD represents the dimensionless temperature standard deviation; T_j is the temperature of each cell in the cross-section; T_a is the average temperature of the cross-section; T_0 represents the temperature of the hot refrigerant; T_i is the temperature of the cold refrigerant; VSD denotes the dimensionless velocity standard deviation; V_j is the velocity of each cell in the cross-section; V_a is the average velocity at the cross-section; V_0 is the velocity of the hot refrigerant and N is the number of cells in the cross-section.

Sensitivity of the grid size is also checked prior to detailed simulations. In the analysis of vertical injections, four cell numbers, 24,776, 47,446, 100,116 and 214,752 are tested for the hole-injection type. Fig. 4 shows the standard deviations of the cross-sectional temperature and velocity downstream of the hole subject to the influence of grid size. It can be seen from the calculated results that a cell number of 100,116 suffice. The largest deviation between cell number of 100,116 and of 214,752 is less than 3%. There is no apparent improvement with doubling the number of cells. Therefore, 100,116 cells for the computation of hole-injection type are used in this study.

3. Results and discussion

Table 1 tabulates the influence of different injection angles and injection velocities on the pressure loss coefficient of the intercooler. The intercooler's pressure loss is directly related to the inlet pressure of the second compression stage. This parameter has a significant influence on the overall performance of the system. Normally a large injection velocity requires a large injected pressure and will lead to a large pressure mixing loss in intercooler. For the same injection angle, the influence of injection velocity on the pressure loss coefficient is comparatively pronounced for a slot injection than for a hole-injection condition. This is attributable to a larger influence zone caused by the slot injection compared to a localized hole-injection. For further examination of the large pressure loss, one can see a typical disordered flow field caused by the lateral impact of the cold refrigerant on the hot refrigerant as shown in Fig. 5a and b. Apparently a greater impact velocity results in a bigger flow separation area as clearly illustrated in Fig. 5b. The size of the flow separation area is strongly connected to the injection angle. A vertical injection arrangement causes the largest lateral impact on the main stream, leading to a large flow separation area. By contrast, more tilted injection angles generate a weaker lateral impact, thus producing a less effect on hot refrigerant flow.

Fig. 6 shows the effect of injection angle on the TSD and VSD, respectively for the slot-injection type at

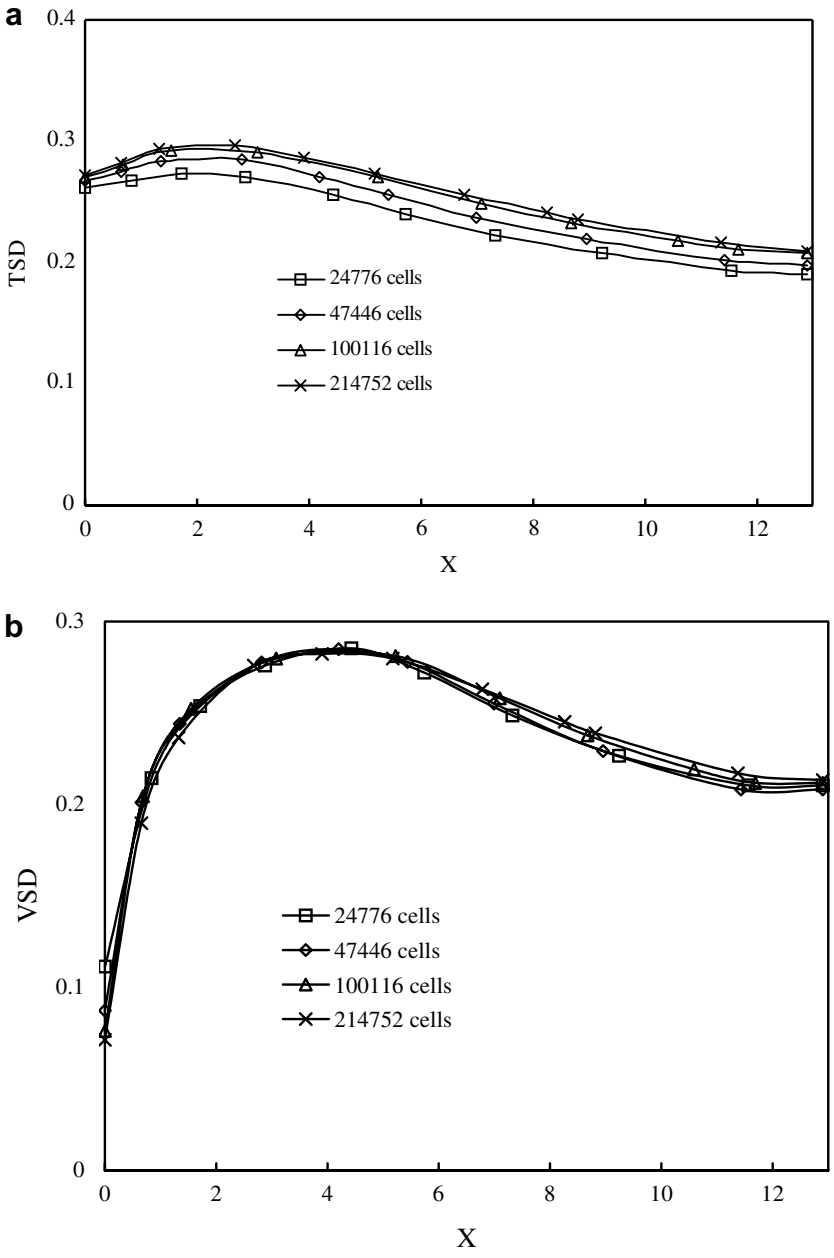

Fig. 4. Grid test results for (a) TSD and (b) VSD.

$V_i/V_0 = 0.63$. In Fig. 6a, the temperature non-uniformity is first increased and reaches a maximum at $X \approx 3$ and decreases thereafter. This phenomenon becomes more pronounced with the rise of the injection angle. As seen in the figure, the variation of temperature non-uniformity along the main stream changes dramatically for the case of vertical injection. Both the highest and lowest non-uniformity occurs at $\theta = 90°$. Conversely, the level of temperature non-uniformity remains fairly unchanged at $\theta = 45°$. However, irrespective of the violent flow field caused by the vertical injection, one should notice that the temperature non-uniformity of $\theta = 45°$ is greater than other injection angles at further downstream ($X > 9$). As seen in Fig. 5a, for a larger injection angle, cold refrigerant with higher momentum rush into the hot refrigerant. It creates a highly disordered flow, composing of flow separation and a non-uniform temperature distribution. In the mean time, the

Table 1
The influence of different injection angles and velocities on pressure loss coefficient of intercooler, Cd

	Slot-injection		Hole-injection	
	$V_i/V_0 = 0.63$	$V_i/V_0 = 1$	$V_i/V_0 = 0.63$	$V_i/V_0 = 1$
$\theta = 90°$	0.460	0.954	0.391	0.581
$\theta = 75°$	0.358	0.686	0.329	0.464
$\theta = 60°$	0.289	0.420	0.254	0.384
$\theta = 45°$	0.246	0.310	0.224	0.326

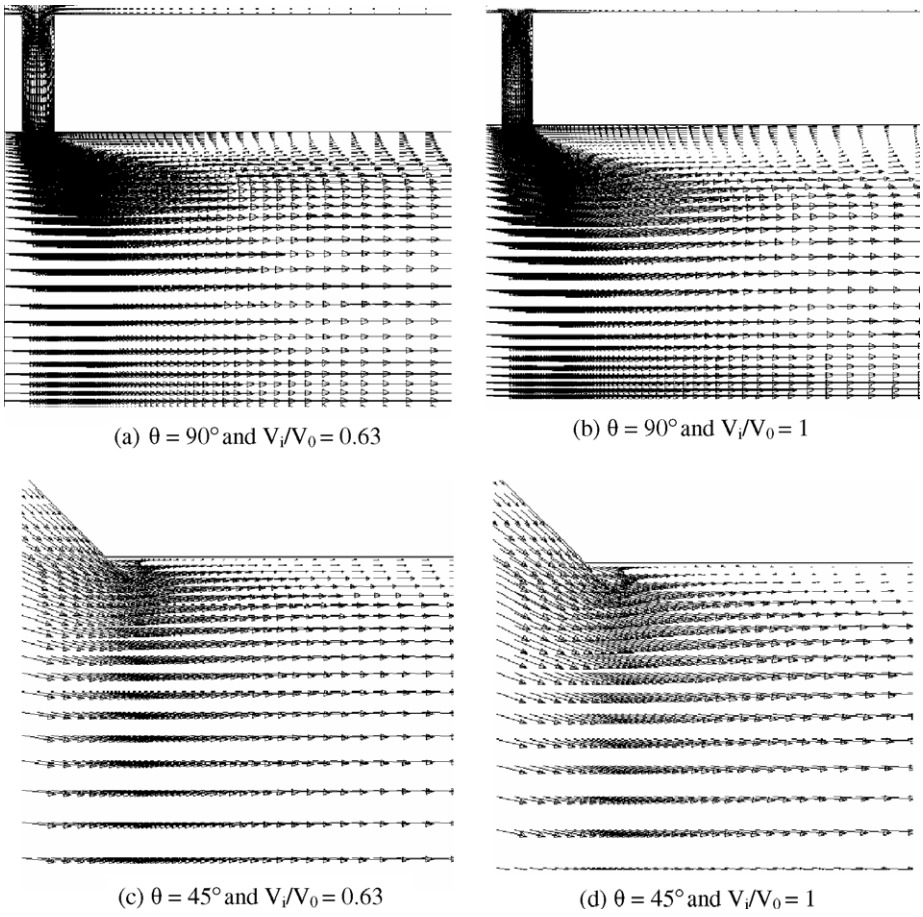

Fig. 5. The flow separation zones under different injection velocities and angles.

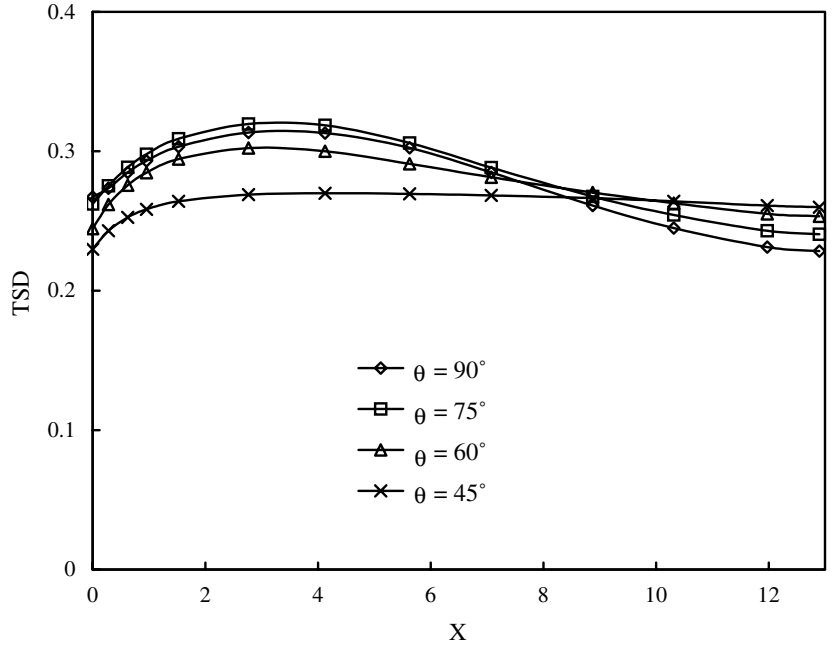

Fig. 6a. Effect of injection angles on TSD for slot-injection type at $V_i/V_0 = 0.63$.

turbulent intensity in the flow separation region is several hundreds times larger than other regions. In this situation, it creates a favorable condition for sufficient mixing of cold and hot refrigerant. This continuous mixing leads to a more

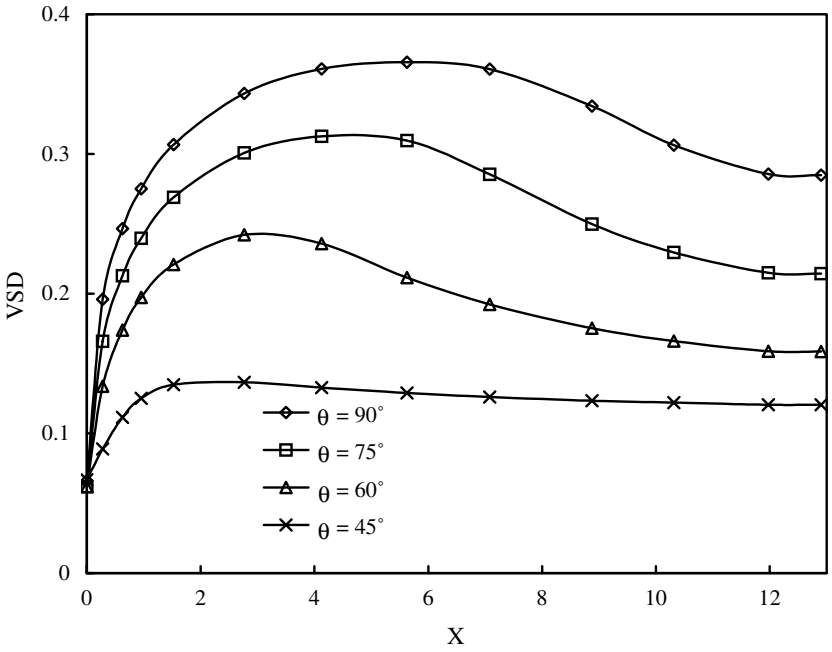

Fig. 6b. Effect of injection angles on VSD for slot-injection type at $V_i/V_0 = 0.63$.

uniform cross-sectional temperature distribution when flow separation ends (or flow reattaches wall). As the injection angle becomes more tilted, the injected cold refrigerant mainly stays at the top portion and the mixing only occurs at the interface of hot and cold refrigerant (shown in Fig. 5c). This leads to an inadequate blending, thereby showing a nearly unchanged non-uniformity of $\theta = 45°$.

Fig. 6b shows the influence of injection angle on the level of velocity non-uniformity for the slot-injection type at $V_i/V_0 = 0.63$. It can be seem from the figure that the level of velocity non-uniformity increases as the injection angle increases. Analogously a larger injection angle may lead to a larger flow separation zone. Eventually larger flow separation gives rise to severe velocity non-uniformity. As the mixing streams flowing further downstream, the velocity non-uniformity decreases due to sufficient momentum mixing of the cold and hot refrigerant and the reattachment of flow separation. In fact, when the injection angle is 45°,

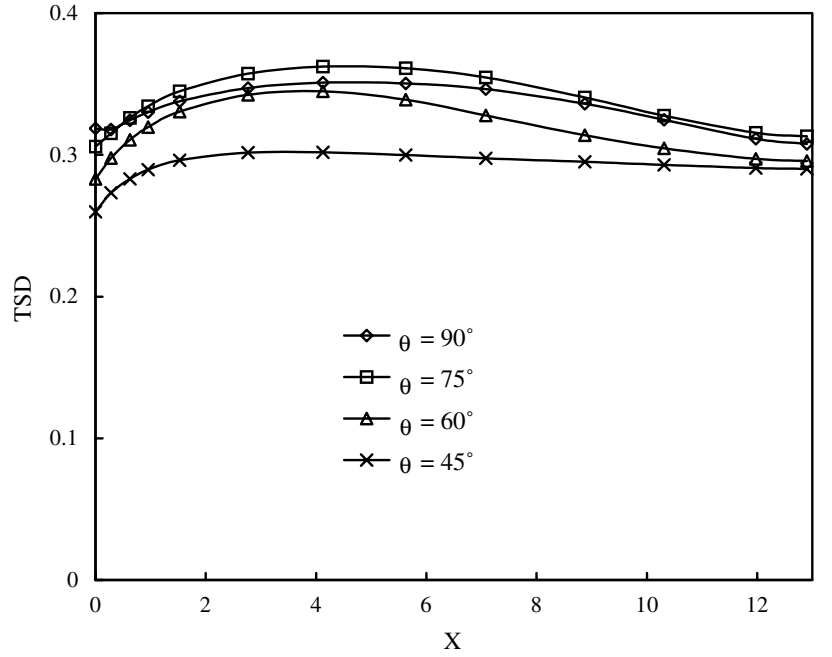

Fig. 7a. Effect of injection angles on TSD for slot-injection type at $V_i/V_0 = 1.0$.

flow separation did not appear (as shown in Fig. 5c). Similarly the cold refrigerant was still limited to the top portion, unable to provide good mixing with hot refrigerant. Hence the level of velocity non-uniformity decreased fairly slowly. Although a tilted injection angle does not provide sufficient momentum mixing, its high uniformity comes from the small difference between the injection velocity and the velocity of the main stream.

Fig. 7a shows the influence of different injection angles on the temperature non-uniformity for the slot-injection type at $V_i/V_0 = 1.0$. When the cold refrigerant is injected into the hot refrigerant with a higher velocity, it introduces a larger velocity component in the direction perpendicular to the mainstream. As a result, larger flow separation zone (shown in Fig. 5b) is encountered where it leads to an amplification of the temperature non-uniformity. The influence of flow separation is greater on velocity than on temperature and the degree of velocity non-uniformity will increase as the flow separation zone is increased. Fig. 7b shows large velocity non-uniformity after the injection of cold refrigerant. Note that the degree of velocity non-uniformity is much higher than those shown in Fig. 6. The flow separation does not occur when $V_i/V_0 = 0.63$ at $\theta = 45°$. However, the occurrence of flow separation starts to appear when $V_i/V_0 = 1.0$ at $\theta = 45°$ (Fig. 5c and d). Therefore, velocity non-uniformity of $V_i/V_0 = 1.0$ is higher than $V_i/V_0 = 0.63$.

Fig. 8a shows the influence of injection angle on the temperature non-uniformity having hole-injection at $V_i/V_0 = 0.63$ whereas Fig. 8b shows the corresponding influence on the velocity non-uniformity. The trend of non-uniform distribution for a hole-injection type at $V_i/V_0 = 0.63$ is quite similar to that of a slot-injection type. However, the temperature and velocity non-uniformity is lower than that of a slot-injection type. It can be seen that slot-injection has a 2-D flow pattern whereas hole-injection has a 3-D flow pattern. A secondary flow occurs in the cross-section consisting of a 3-D flow motion as shown in Fig. 9. The value of isothermal contour is defined as $(T - T_i)/(T_0 - T_i)$. The occurrence of secondary flow results from the lateral flow injecting into the main flow. The vertical velocity component increases as the injection angle is being increased, leading to a stronger secondary flow at a larger injection angle. This secondary flow can create the non-uniformity, and provide good mixing between the hot and cold refrigerant. In fact, the cold refrigerant can then be easily merged into the main flow field, while the high temperature and high velocity refrigerant can be delivered into the cold refrigerant area. A noticeable swirled motion is generated and moves toward the downstream of the intercooler under the present hole-injection arrangement. This provides a room for good mixing between hot and cold refrigerant. In that sense, the non-uniformity of the temperature and velocity for the hole-injection type is considerably lower than that of the slot-injection.

Fig. 10a shows the influence of various injection angles on temperature non-uniformity for a hole-injection type at $V_i/V_0 = 1$. Fig. 10b shows the influence of various injection angle on velocity non-uniformity for a hole-injection type when $V_i/V_0 = 1$. When the injection velocity increases, not only flow separation zone is increased further but also the secondary flow becomes more vivid due to a higher vertical velocity component. By comparing Fig. 9 with Fig. 7, it can be concluded that the hole-injection type has a significant improvement over the slot-injection type at $V_i/V_0 = 1$

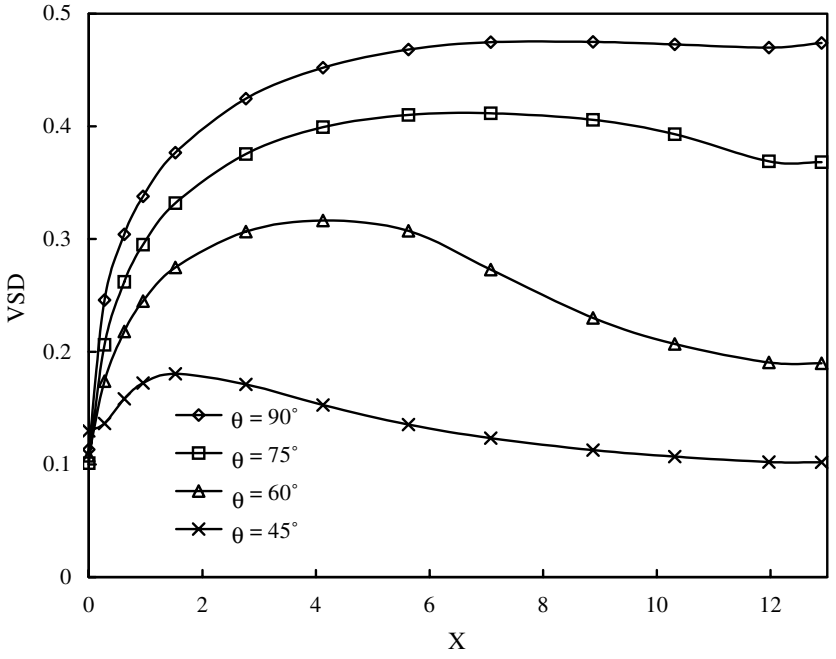

Fig. 7b. Effect of injection angles on VSD for slot-injection type at $V_i/V_0 = 1.0$.

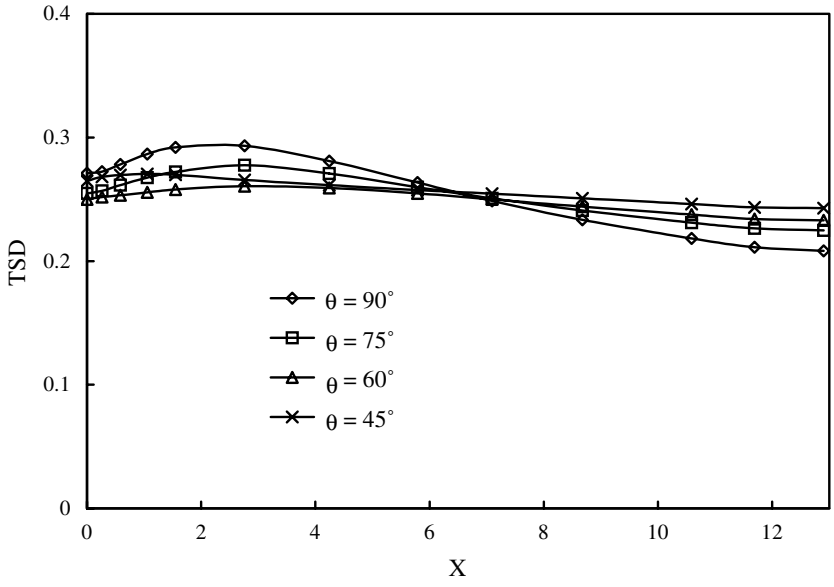

Fig. 8a. Effect of injection angles on TSD for hole-injection type at $V_i/V_0 = 0.63$.

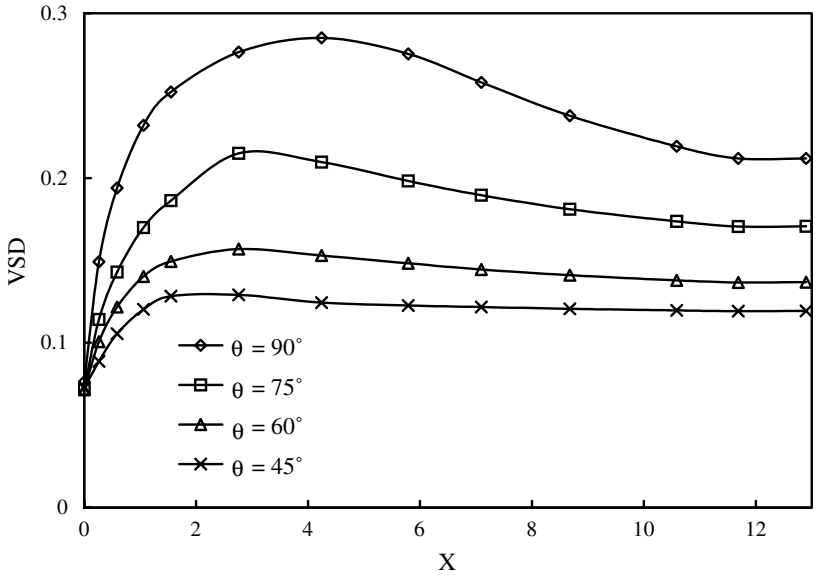

Fig. 8b. Effect of injection angles on VSD for hole-injection type at $V_i/V_0 = 0.63$.

in terms of uniformity of the temperature and velocity distribution. However, the difference in non-uniformity is reduced when V_i/V_0 is reduced to 0.63. From Fig. 10, the velocity non-uniformity is increased due to a huge flow separation at the beginning but its strength dies down quickly due to the strong secondary flow, suggesting that the injection velocity is not a dominant variable in the design of the hole-injection type intercooler.

In conclusion, when a slot-injection type intercooler is chosen, a high flow velocity of cold refrigerant injection is not desirable. This is because it equipped with a higher pressure loss, and pronounced non-uniformity of temperature and velocity in the intercooler. The secondary flow appeared in the hole-injection type intercooler can reduce the temperature and velocity non-uniformity caused by the injected cold refrigerant. Even though the intercooler's pressure loss will increase for high velocity injection case, it is not so significant in a slot-injection type.

4. Conclusions

This study analyzed the thermal and flow fields of an intercooler in a two-stage refrigeration compressor using numerical method. The effect of inject types, namely the

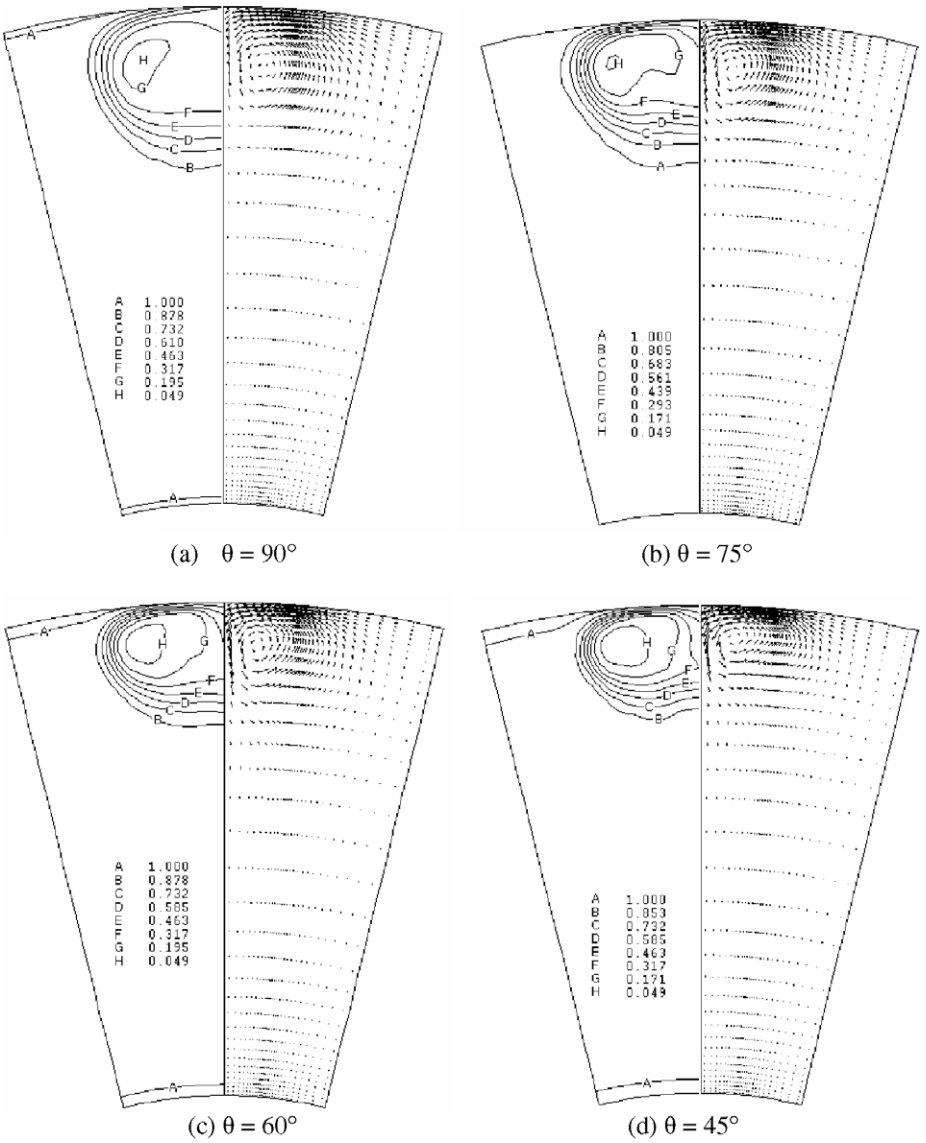

Fig. 9. The secondary flow on the cross-section vertical to mainstream direction ($X = 5$). The right hand side of each diagram denotes velocity vectors whereas the left hand side represents a diagram of isothermal contours.

slot-injection and hole-injection, on the overall mixing characteristics of intercoolers are investigated. The angle and ejected velocity of the cold refrigerant are the major variable parameters being examined. Based on the aforementioned discussions, the following conclusions are drawn:

1. When the injection angle is large, the pressure loss of the intercooler will rise, which are associated with the flow separation. When the injection velocity is increased, the pressure loss also rises. The pressure loss of hole-injection type is lower than that of the slot-injection type.
2. Larger injection angles provide better temperature mixing of the refrigerant, where the level of temperature non-uniformity increases first along the flow direction and levels off rapidly when it reaches a maximum. Smaller injection angles lead to a poor temperature mixing of the refrigerant, where the level of the temperature non-uniformity decreases fairly slowly.
3. Larger injection angles generate bigger flow separation zones which results in velocity non-uniformity, whereas smaller injection angles give rise to a less velocity non-uniformity.
4. As the injection velocity rises, both the temperature and velocity non-uniformity of the slot-injection type increase significantly whereas the injection velocity has negligible influence on the relevant uniformity for a hole-injection type.
5. For the same injection velocity, the existence of secondary flow in the hole-injection type is more beneficial when compared to the slot-injection type. The advantages become even more apparent during high injecting flow rates.

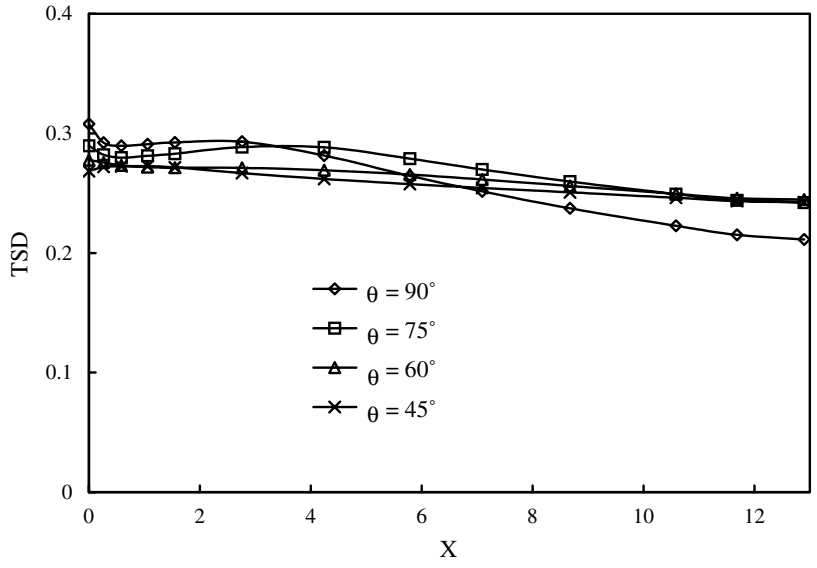

Fig. 10a. Effect of injection angle on TSD for hole-injection type at $V_i/V_0 = 1$.

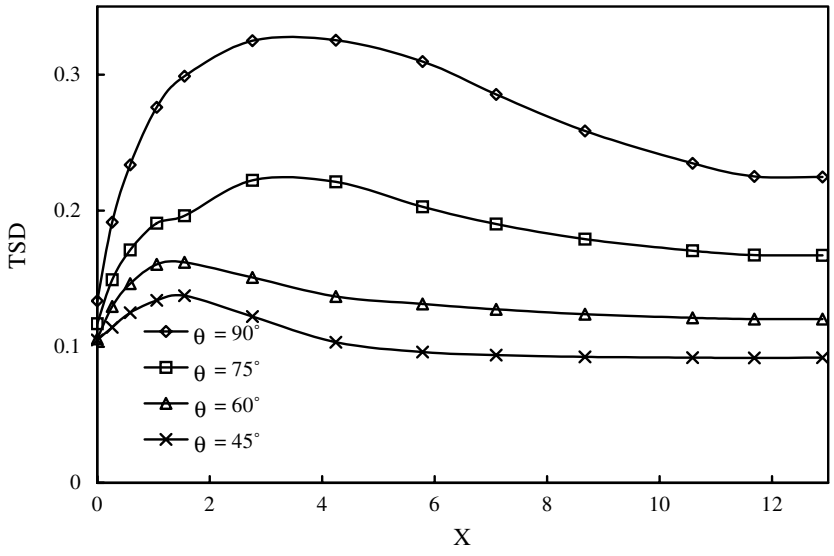

Fig. 10b. Effect of injection angle on VSD for hole-injection type at $V_i/V_0 = 1$.

6. Taking into consideration the uniformity of both the velocity and the temperature distribution, it is recommended to use the hole-injection type of intercooler with an injection angle of 60°.

Acknowledgement

The last author would like to appreciate some financial support from the Bureau of Energy, ministry of economic affairs, Taiwan.

References

[1] A.D. Fitt, J.R. Ockendon, T.V. Jones, Aerodynamics of slot-film cooling: theory and experiment, Journal of Fluid Mechanics 160 (1985) 15–27.

[2] R.J. Goldstein, Film cooling on a gas turbine blade near the end wall, ASME Journal of Engineering for Gas Turbine and Power 107 (1985) 117–122.

[3] P.M. Ligrani, Adiabatic film cooling effectiveness from heat transfer measurement in compressible, variable-property flow, ASME Journal of Heat Transfer 107 (1985) 313–320.

[4] P.M. Ligrani, C.S. Subramanian, D.W. Craig, P. Kaisuwan, Effect of vorticities with different circulations on heat transfer and injectant downstream of a single film cooling hole in a turbulent boundary layer, ASME Journal of Turbomachinery 113 (1991) 433–441.

[5] S.G. Schwarz, R.J. Goldstein, Two-dimensional behavior of film cooling jet on concave surface, ASME Journal of Turbomachinery 111 (1989) 124–130.

[6] P.M. Ligrani, S.W. Mitchell, Effects of embedded vortices on injectant from film cooling holes with large spanwise spacing and compound angle orientations in a turbulent boundary layer, ASME Journal of Turbomachinery 116 (1994) 709–720.

[7] S.V. Ekkad, D. Zapata, J.C. Han, Film effectiveness over a flat surface with air and CO_2 injection through compound angle holes using a transient liquid crystal image method, ASME Journal of Turbomachinery 119 (1997) 587–593.
[8] H. Nasir, S.V. Ekkad, S. Acharya, Effect of compound angle injection of flat surface film cooling with large streamwise injection angle, Experimental Thermal and Fluid Science 25 (2001) 23–29.
[9] Y.L. Lin, T.I.P. Shih, Film cooling of a cylindrical leading edge with injection through rows of compound-angle holes, ASME Journal of Heat Transfer 123 (2001) 645–654.
[10] H.W. Lee, J.J. Park, J.S. Lee, Flow visualization and film cooling effectiveness measurements around shaped holes with compound angle orientations, International Journal of Heat and Mass Transfer 45 (2002) 145–156.
[11] B.Y. Maiteh, B.A. Jubran, Effects of pressure gradient on film cooling effectiveness from two rows of simple and compound angle holes in combination, Energy Conversion and Management 45 (2004) 1457–1469.
[12] C.H.N. Yuen, R.F. Martinez-Botas, Film cooling characteristic of a single round hole at various streamwise angle in a crossflow: part I effectiveness, International Journal Heat and Mass Transfer 46 (2003) 221–235.
[13] P.M. Ligrani, R. Gong, J.M. Cuthrell, J.S. Lee, Bulk flow pulsations and film cooling – I. Injectant behavior, International Journal of Heat and Mass Transfer 39 (1996) 2271–2282.
[14] P.M. Ligrani, R. Gong, J.M. Cuthrell, J.S. Lee, Bulk flow pulsations and film cooling – II flow structure and film effectiveness, International Journal of Heat and Mass Transfer 39 (1996) 2283–2292.
[15] P.M. Ligrani, R. Gong, J.M. Cuthrell, Bulk flow pulsations and film cooling: flow structure just downstream of the holes, ASME Journal of Turbomachinery 119 (1997) 568–573.
[16] I.S. Jung, J.S. Lee, P.M. Ligrani, Effects of bulk flow pulsations on film cooling with compound angle holes: heat transfer coefficient ratio and heat flux ratio, ASME Journal of Turbomachinery 124 (2002) 142–151.
[17] J.S. Lee, I.S. Jung, Effect of bulk flow pulsations on film cooling with compound angle holes, International Journal of Heat and Mass Transfer 45 (2002) 113–123.
[18] V.P. Lebedev, V.V. Lemanov, S.Ya. Misyura, V.I. Terekhov, Effect of flow turbulence on film cooling efficiency, International Journal of Heat and Mass Transfer 35 (1995) 2117–2125.
[19] Y.J. Kim, S.M. Kim, Influence of shaped injection holes on turbine blade leading edge film cooling, International Journal Heat and Mass Transfer 47 (2004) 245–256.
[20] A.A. Amer, B.A. Jubran, M.A. Hamdan, Comparison of different two-equation turbulence models for prediction of film cooling from two rows of holes, Numerical Heat Transfer Part A: Applications 21 (1992) 143–162.
[21] M. Kadja, G. Begeles, Computational study of turbine blade cooling by slot-injection of a gas, Applied Thermal Engineering 17 (1997) 1141–1149.
[22] J. Bellettre, F. Bataille, A. Lallemand, Prediction of thermal protection of walls by blowing with different fluids, International Journal of Thermal Science 38 (1999) 492–500.
[23] D. Lakehal, G.S. Theodoridis, W. Rodi, Three-dimensional flow and heat transfer calculations of film cooling at the leading edge of a symmetrical turbine blade model, International Heat and Fluid Flow 22 (2001) 113–122.
[24] S. Thakur, J. Wright, W. Shyy, Convective film cooling over a representative turbine blade leading edge, International Journal Heat and Mass Transfer 42 (1999) 2269–2285.
[25] V.K. Garg, R.L. Gaugler, Effect of coolant temperature and mass flow on film cooling of turbine blade, International Journal of Heat and Mass transfer 40 (1997) 435–445.
[26] V.K. Garg, Heat transfer on a film-cooled rotating blade using different model, International Journal Heat and Mass transfer 42 (1999) 789–802.
[27] I. Koc, C. Parmaksizoglu, M. Cakan, Numerical investigation of film cooling effectiveness on the curved surface, Energy Conservation and Management 47 (2006) 1231–1246.
[28] X. Guo, W. Schroder, M. Meinke, Large-eddy simulations of film cooling flows, Computers and Fluid 35 (2006) 587–606.
[29] J.M. Miao, C.Y. Wu, Numerical approach to hole shape effect on film cooling effectiveness over flat plate including internal impingement cooling chamber, International Journal Heat and Mass Transfer 49 (2006) 919–938.